High adsorption capacity of Rhodamine B dye on bio-activated carbon derived from sugarcane bagasse

Nguyen Thi Thu Hang[(1)], Nguyen Kim Thuy[(1)], Vu Minh Chau[(1)], Cao Phuong Anh[(1)], Han Duy Linh[(1)], Dang Minh Quang[(1)], Dao Duy Khanh[(2)], Duong Tuan Hung[(2)], Nguyen Thi Hoai Phuong[(1)*]

[(1)]*Department of Chemistry and Environment, Joint Vietnam-Russia Tropical Science and Technology Research Center, 63 Nguyen Van Huyen stress, Nghia Do ward, Hanoi, Vietnam*

[(2)]*Institute of Chemistry, Vietnam Academy of Science and Technology, 18 Hoang Quoc Viet, Hanoi, Vietnam*

[*]*Corresponding author: - Nguyen Thi Hoai Phuong*

- Address: 63 Nguyen Van Huyen stress, Nghia Do ward, Hanoi, Vietnam

- Phone: +84 975482730; Email: hoaiphuong1978@gmail.com

- Highlights:

- ✓ Bio-activated carbon derived from sugarcane bagasse achieves >95% Rhodamine B removal within 10–20 minutes, demonstrating fast adsorption kinetics and high affinity.
- ✓ Adsorption follows a pseudo-second-order kinetic model and fits best with the Freundlich isotherm, indicating chemisorption on heterogeneous surfaces with multilayer formation.
- ✓ The adsorbent exhibits a high q_{max} of 30.36 mg g^{-1}, with a mesoporous structure and oxygen-rich functional groups, promoting sustainable valorization of agro-industrial sugarcane waste.

- Abstract: This paper details the synthesis, characterisation, and adsorption efficacy of bio-activated carbon (BAC) generated from sugarcane bagasse for the effective elimination of Rhodamine B (RhB) dye from aqueous solutions. Sugarcane bagasse, an accessible agro-industrial byproduct, was chemically activated with HCl and subsequently carbonized to yield a porous carbon material rich in surface functionalities. Structural and surface analyses validated the formation of a hierarchical mesoporous framework, as demonstrated by SEM, FTIR, XRD, EDX, and nitrogen adsorption–desorption tests, including predominant pore sizes within the 2–5 nm range and intact oxygenated groups conducive to dye adsorption. Batch adsorption tests exhibited fast elimination of RhB, reaching equilibrium in 20 minutes and sustaining removal efficiencies over 95% across a broad concentration spectrum. Kinetic modeling indicated that the pseudo-second-order model most accurately represented the adsorption process, emphasizing chemisorption as the primary mechanism, with heterogeneous surface interactions and pore diffusion effects. Isotherm analysis revealed that the Freundlich model exhibited the optimal fit (R^2 = 0.9950), indicating multilayer adsorption on energetically heterogeneous sites, with a maximum adsorption capacity (q_{max}) of 30.36 mg g^{-1} as determined by the Langmuir model. Further fittings to the Temkin, Elovich, Henry, and Dubinin–Radushkevich models corroborated a synthesis of physical and chemical adsorption

mechanisms. The findings validate that sugarcane-bagasse-derived BAC is an economical, sustainable, and efficient adsorbent, presenting considerable promise for practical wastewater treatment applications while facilitating the valorization of agricultural residues into valuable environmental remediation materials.

- Keywords: *Bio-activated carbon, sugarcane bagasse, rhodamine B removal, adsorption isotherms and kinetics, waste valorization*

1. INTRODUCTION

The textile industry is one of the biggest users of the dyes and accounts for 70% of its market generates approximately one trillion dollars, accounts for 7% of total global exports, and employs approximately 35 M people worldwide [1, 2]. The textile industries are associated with discharge huge quantities of the dye wastewater which are resulted from the washing textiles, coloured or the printed fabrics. The reports indicated that 40,000 industrial synthetic dyes are actively generating 450,000 tons (t) of the dyes annually [3]. One of the most toxic dyes in textile wastewater is Rhodamine B (RhB) which has an extensive value in the textile industry as textile colourant because of its high stability and non-biodegradable [4]. RhB is a synthetic cationic xanthene dye extensively utilized in the textile, printing, and cosmetic sectors [5]. Nonetheless, its discharge into aquatic environments presents significant ecological hazards, including persistence in aquatic ecosystems, phototoxicity, and possible carcinogenic and neurotoxic consequences [4, 6]. Traditional treatment methods, such as coagulation, advanced oxidation, and membrane filtration, can entail significant operational expenses, produce detrimental byproducts, and need intricate infrastructure [7-9]. These gaps offer the opportunity for the researchers to find more efficient technologies for improving the quality of textile wastewater treatment before the final discharge into the environment. Adsorption, especially via activated carbon, has proven to be an effective, adaptable, and eco-friendly method for the elimination of dye pollutants from aqueous solutions (e.g., recent extensive reviews of RhB treatment technologies) [10-12]. Activated carbon (AC) is a widely used material for electrochemical, energy, and environmental applications due to its low cost, large surface area typically ranging from 500 to over 3000 m^2 g^{-1}, and developed porous structure with a pore system comprising micropores (< 2 nm), mesopores (2–50 nm), and macropores (> 50 nm), which helps increase its adsorption capacity and chemical reactivity on the surface. However, conventional activated carbon production using coal or petroleum-derived feedstocks is resource-intensive and less sustainable [13-15].

Amid the worsening global environmental pollution and the ongoing energy crisis, the development of sustainable and environmentally benign materials has become a critical research priority. In this context, bio-based activated carbon (Bio-AC), derived from renewable biomass resources such as bark, rice husk, corn cobs, coffee husks, and sugarcane bagasse, has gained considerable attention as an emerging generation of high-performance adsorbents. Owing to its wide availability, low production cost, and tunable physicochemical properties, Bio-AC offers a

compelling alternative to conventional activated carbons for environmental remediation applications. AC made from agricultural wastes is considered more efficient due to the high efficiency of removing dyes effortlessness and no hazardous by-products. Conversely, sugarcane bagasse, a byproduct of the sugar and bioethanol industries, provides a sustainable, economical, and plentiful biomass source, containing high levels of cellulose (45–55%), hemicellulose (20-25%), and lignin (18-24%) [16-18]. Bagasse is an ideal low-cost raw material for making activated carbon. Numerous studies have shown the effective transformation of sugarcane bagasse into activated carbon with comparable porosity and adsorption efficacy via chemical or physical activation techniques [19-21].

While activated carbon from sugarcane bagasse has demonstrated effectiveness in adsorbing dyes such as Rhodamine B and heavy metals, research specifically focused on the removal of RhB using bio-activated carbon from the green-skin fraction of sugarcane bagasse is scarce [22-24]. This work contributes significant new insights into the unexploited potential of sugarcane green-skin waste, advances a sustainable route to high-performance activated carbon, and establishes a robust adsorption mechanism for RhB removal. These contributions highlight the feasibility of converting underutilized agro-industrial residues into functional materials for wastewater remediation, supporting both environmental sustainability and circular resource utilization.

2. EXPERIMENTAL

2.1. Materials and reagents

Rhodamine B (RhB, ≥ 99%), potassium hydroxide (KOH, pellets), hydrochloric acid (HCl, 37%), sodium hydroxide (NaOH, pellets), sodium chloride (NaCl, > 99.5%), and ethanol (C_2H_5OH, ≥ 99.5%) were of analytical grade and utilized as received. Pure water was utilized consistently. Fresh sugarcane bagasse (SCB) was procured from a local juice press, meticulously cleaned with tap water followed by deionized water to eliminate residual sugars and particulates, and subsequently air-dried.

2.2. Preparation of bio-activated carbon (BAC)

The process of preparing BAC is shown in (Figure 1). The cleaned sugarcane bagasse (SCB) was oven-dried at 105°C for 24 h, milled to ≤ 2 mm, and stored in airtight containers with desiccant. For each batch, 20 g SCB was placed in a quartz boat and heated under nitrogen (100 mL min^{-1}), ramped to 450°C at 10°C min^{-1}, held for 2 h, then cooled. The precursor was impregnated with 10 wt% HCl (HCl:SCB = 1:1, w/w), soaked 24 h at room temperature with intermittent stirring, filtered, rinsed with distilled water to neutral pH, and dried at 105ºC overnight. Impregnated samples were carbonized at 500°C for 60 min in nitrogen (10°C min^{-1}). The product AC was ground to < 200 µm, stored in desiccant vials, and the biochar yield was determined.

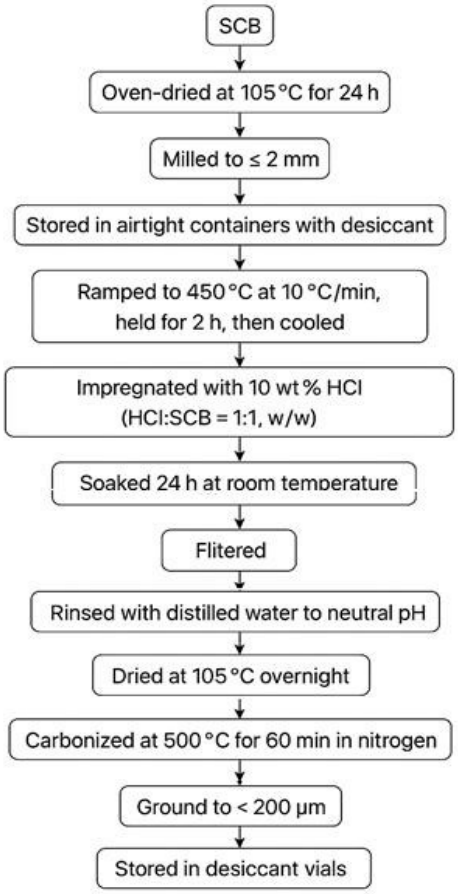

Figure 1: Flowchart showing the process of preparing BAC

2.3. Characterizations

Morphology was analyzed using scanning electron microscopy (SEM). Crystallinity was assessed by X-ray diffraction (XRD) using Cu Kα radiation at 40 kV and 30 mA, over a 2θ range of 10–70°, the phase of the material was closely analyzed at a rate of 5°/min. FTIR infrared spectroscopy was employed to investigate the material's bonds and functional groups in the 400–4000 cm^{-1} wavenumber region. The elemental composition was ascertained using EDX analysis. The textural qualities were assessed using N_2 adsorption-desorption, measuring the BET surface area, pore volume at $P/P_0 = 0.99$, the porosity of the materials was comprehensively examined at 77 K, and pore size distribution (BJH) following degassing at 150°C for 3 hours.

2.4. Batch adsorption experiments

A 1000 mg L^{-1} RhB stock solution was produced in water and stored in the dark at refrigeration temperatures for no more than one week. Daily preparations of

working solutions (5–50 mg L^{-1}) were conducted. UV-Vis spectrophotometry at λmax = 552 nm (confirmed by scanning from 400 to 700 nm) was employed to measure RhB. Calibration curves (minimum of 6 points) exhibited linearity with R^2 values of at least 0.999; blanks (water) and quality control checks (mid-range standards) were conducted every 10 samples. Supernatants were subjected to filtration using 0.22 µm PTFE before to measurement. Unless specified: V = 50 mL, adsorbent dose = 0.5–2.0 g L^{-1} (typically 1.0 g L^{-1}), agitation = 150 rpm in 100 mL Pyrex conical flasks. After contact, suspensions were filtered and analyzed by UV-Vis. Adsorption capacity qt and removal efficiency H were calculated by:

$$q_t = \frac{(C_o - C_t) \times V}{m} \quad (1)$$

$$H = \frac{(C_o - C_t) \times 100}{C_o} \quad (2)$$

q_t (mg g^{-1}) is adsorption capacity at time t; C_o and C_t (mg L^{-1}) are initial and time-t RhB concentrations; V (L) is solution volume; m (mg) is adsorbent mass; H (%) removal efficiency.

Kinetics study: The initial concentration is C_0 = 10 mg L^{-1}, and the dosage is 1.0 g L^{-1}. Aliquots were collected at many time intervals from 0 to 120 minutes, with concentrated early sampling at 10, 20, 30, 40, 50, 60, 90, and 120 minutes. The data will be analyzed using the pseudo-first-order (PFO), pseudo-second-order (PSO), Bangham, and Elovich models. The goodness of fit will be assessed using R^2 values, and the multilinear regions for diffusion will be analyzed.

Isotherm study: Equilibrate solutions at a concentration of 1.0 g L^{-1} for 24 hours, as confirmed by kinetics, utilizing beginning concentrations (C_0) between 5 and 25 mg L^{-1}. Apply non-linear regression to fit the data to the subsequent isotherm models: Langmuir, Freundlich, Temkin, Elovich, Henry, and Dubinin–Radushkevich. Provide the parameters q_{max}, K_L, K_F, and 1/n, together with their respective 90% confidence intervals.

3. RESULTS

3.1. Characterization of bio-activated carbon

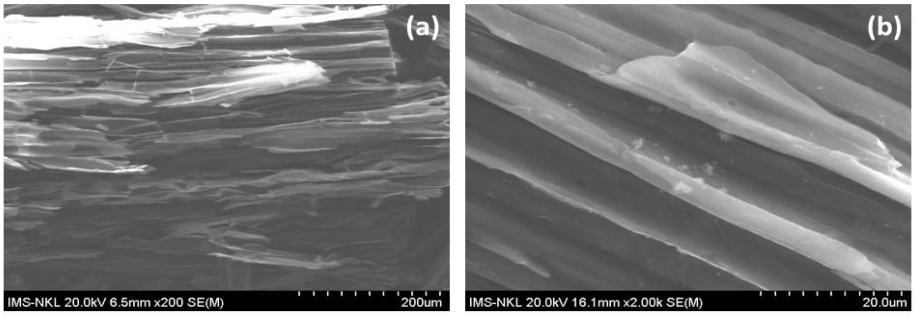

Figure 2. SEM images of bio-activated carbon from sugarcane bagasse

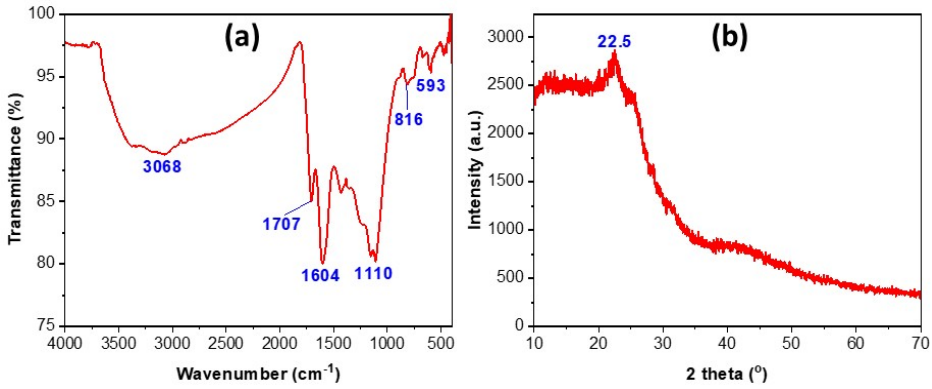

Figure 3. FTIR spectra (a) and XRD pattern (b) of bio-activated carbon from sugarcane bagasse.

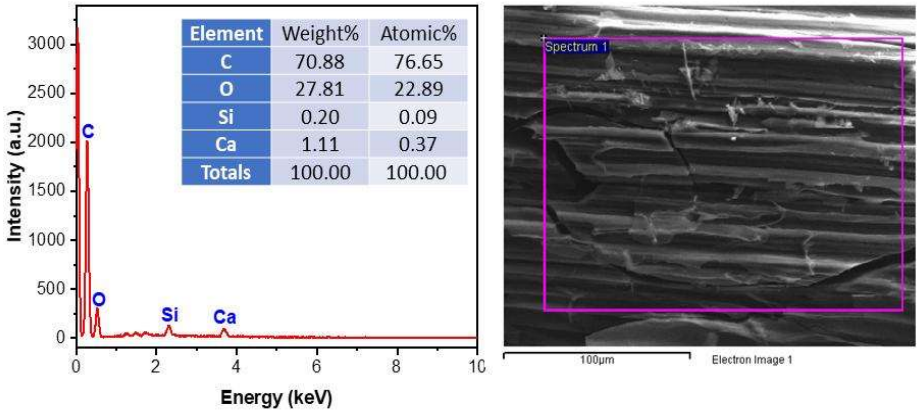

Figure 4. EDX spectra of bio-activated carbon from sugarcane bagasse

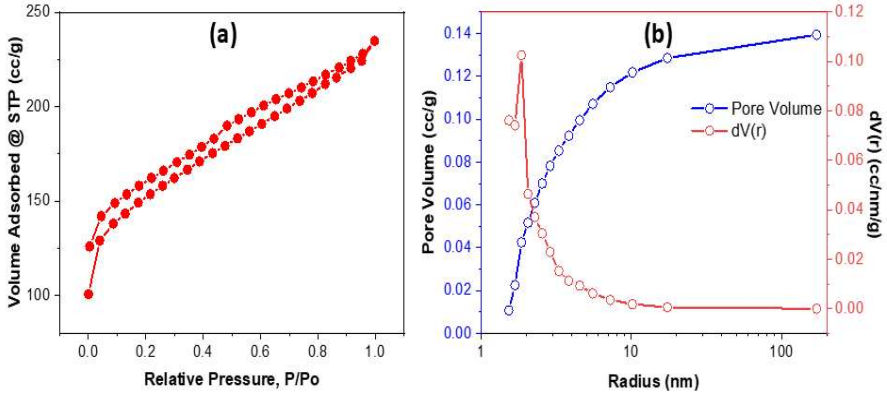

Figure 5. N_2 isotherm (a) and pore size distribution (b) of bio-activated carbon from sugarcane bagasse

3.2. RhB adsorption study

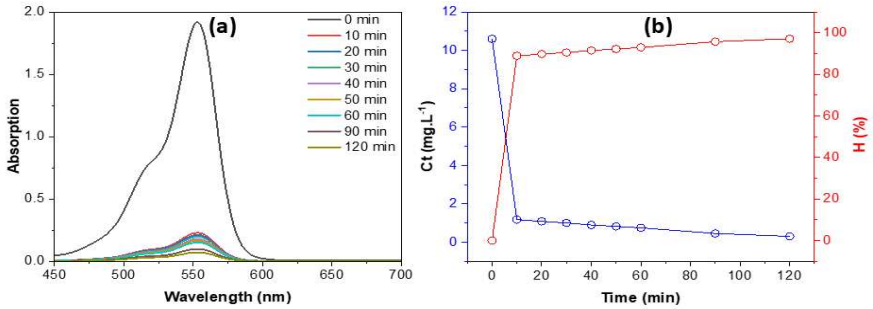

Figure 6. UV-Vis spectra (a), concentration, and removal efficiency (b) of RhB on bio-activated carbon from sugarcane bagasse vs. time

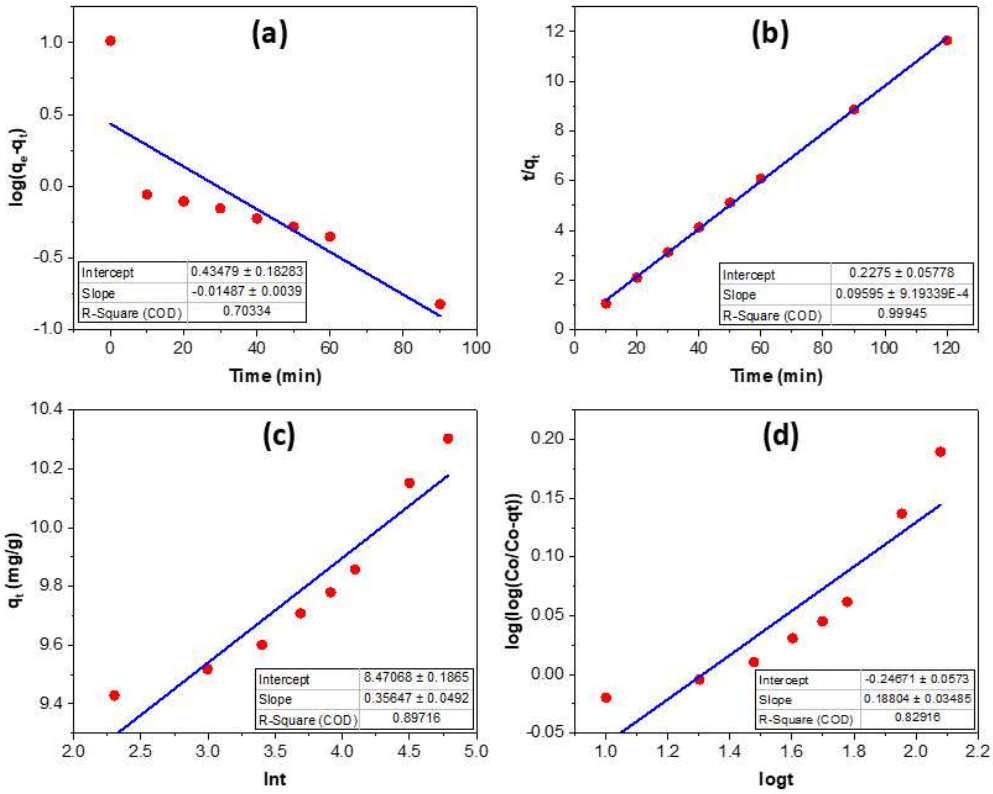

Figure 7. Kinetics of RhB adsorption on bio-activated carbon from sugarcane bagasse: pseudo-first-order (a), pseudo-second-order (b), Elovich (c), and Bangham (d)

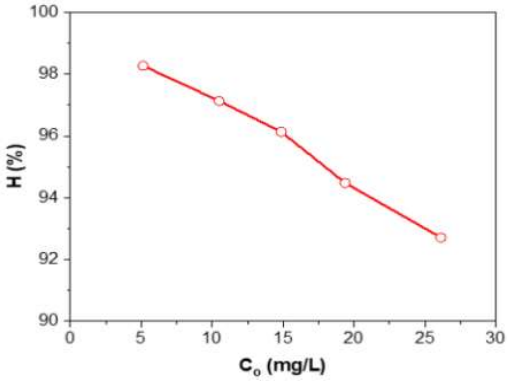

Figure 8. RhB removal efficiency vs. intial concentration by bio-activated carbon from sugarcane bagasse

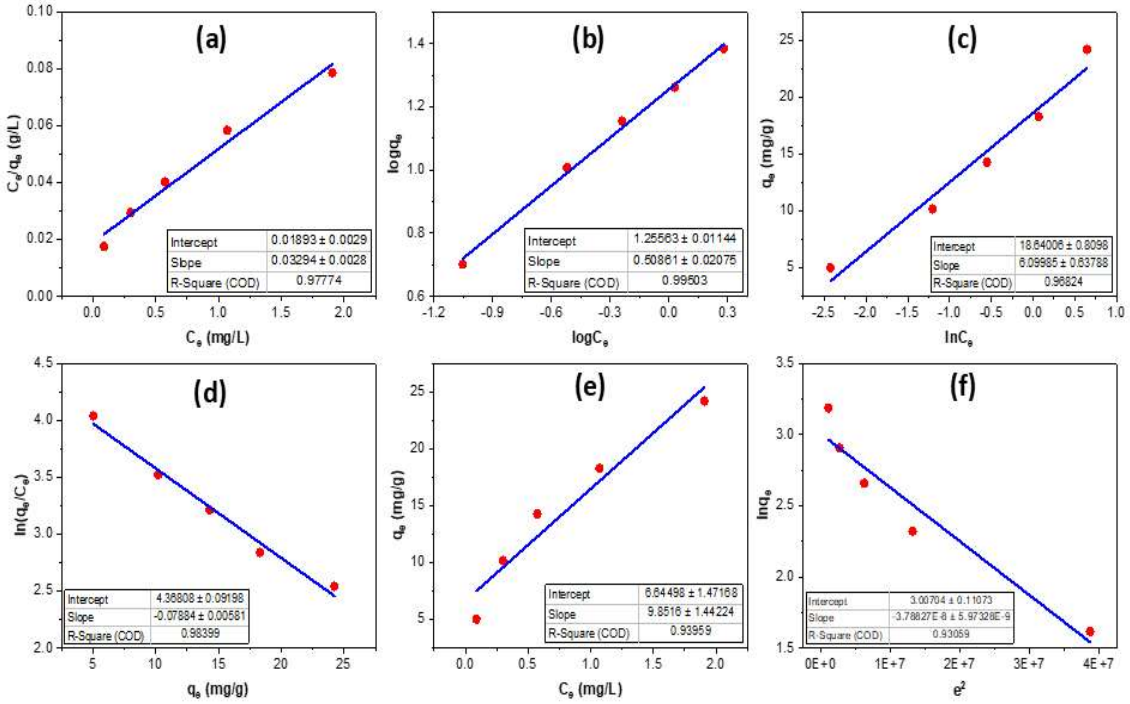

Figure 9. RhB isotherm adsorption on bio-activated carbon from sugarcane bagasse: Langmuir (a), Freudlich (b), Temkin (c), Elovich (d), Henry (e), and Dubinin–Radushkevich (d).

Table 1. Parameters of RhB isotherm adsorption on bio-activated carbon from sugarcane bagasse.

Models	Parameters	Value
Langmuir	K_L (L mg^{-1})	1.74
	q_{max} (mg g^{-1})	30.36
	R^2	**0.9777**
Freundlich	K_F (mg g^{-1}) (L $mg^{-1})^{1/n}$	18.015
	n	1.97
	R^2	**0.9950**
Temkin	K_T (L g^{-1})	21.24
	b_T (J mol^{-1})	6.10
	R^2	0.9682
Elovich	α (mg g^{-1})	78.89
	β (g mg^{-1})	0.0788
	R^2	0.9840
Henry	K_H (L g^{-1})	9.8516
	R^2	0.9396
Dubinin–Radushkevich	q_{max} (mg g^{-1})	20.24
	β (mol^2 kJ^{-2})	$3.79x10^{-8}$
	E (kJ mol^{-1})	3.63
	R^2	0.9306

Table 2. Maximum monolayer adsorption capacity and surface area of different agricultural wastes for RhB.

Adsorbent used	Dye used	Q_{max} (mg g^{-1})	Surface area (m^2 g^{-1})	References
Cotton stalks	Rhodamine B	144.36	461	[30]
Palm tree bark	Rhodamine B	31.81–224.30	189.157	[31]
Walnut shells	Rhodamine B	1.451–2.292	474.38–815.60	[32]
Lemongrass essential-oil distillation residue	Rhodamine B	14.93	18.3	[33]
Sugarcane bagasse	Rhodamine B	30.36	473.5	This study

4. DISCUSSION

4.1. Characterization of bio-activated carbon

Figure 2 presents SEM pictures that illustrate the morphological features of bio-activated carbon obtained from sugarcane bagasse. At low magnification (a), the material displays a stratified and uneven architecture with superimposed carbon sheets, signifying the partial retention of the fibrous framework of the predecessor. The layers are loosely organized, resulting in interstitial spaces that can promote adsorptive interactions. At increased magnification (b), the surface is more distinct, revealing elongated, smooth, and aligned carbon structures interspersed with occasional cracks and pores. The activation method improved surface roughness and created porosity, both essential for augmenting surface area and adsorption capacity, rendering the bio-activated carbon appropriate for environmental remediation applications.

Overall, the SEM images confirm that sugarcane-bagasse-derived activated carbon retains a hierarchical porous structure combining macroporous channels with layered microstructures. Such morphology is advantageous for environmental remediation, as it promotes fast adsorption, large accessible surface area, and efficient interaction between pollutants and the carbon framework.

The FTIR spectrum (Figure 3a) of activated carbon synthesized from sugarcane bagasse reveals several characteristic absorption bands, confirming the presence of functional groups typically associated with lignocellulosic-derived carbon materials. The weak band in the range of 3000–3200 cm^{-1} is attributed to residual O–H stretching vibrations, originating from hydroxyl groups in cellulose, hemicellulose, or surface-adsorbed water. The peak at 1707 cm^{-1} corresponds to C=O stretching of carbonyl and carboxyl functional groups, indicating partial oxidation during activation. Such oxygen-containing groups are known to enhance the hydrophilicity and adsorption affinity of activated carbon toward polar contaminants. The band at 1604 cm^{-1} are associated with aromatic C=C stretching, reflecting the development of conjugated carbon structures during pyrolysis. The sharp band at 1110 cm^{-1} is characteristic of C–O–C stretching in ether or alcohol groups, typically retained from the lignocellulosic matrix. The low-frequency peaks at ~816 cm^{-1} and ~593 cm^{-1} correspond to out-of-plane C–H bending and deformation vibrations of aromatic rings, further confirming the formation of an aromatic carbon network [25, 26]. The XRD pattern (Figure 3b) often exhibits two broad diffraction peaks at $2\theta = 22.5°$ (graphitic (002)), indicating low crystallinity and the existence of amorphous carbon [27]. These spectral and structural characteristics align with previously published research on activated carbons derived from sugarcane bagasse. The absence of sharp, well-defined peaks indicates that the carbon framework lacks long-range order. Such structural disorder is typical of activated carbon synthesized from biomass precursors and is advantageous for adsorption applications due to: A high density of defect sites; Increased surface reactivity and a large distribution of micro-and mesopores. The gradual decrease in intensity toward higher angles further supports the amorphous nature of the material.

The EDX spectrum of bio-activated carbon derived from sugarcane bagasse (Figure 4) indicates that carbon and oxygen are the predominant elements, comprising 70.88 wt% (76.65 at%) and 27.81 wt% (22.89 at%), respectively, which aligns with the lignocellulosic nature of the precursor. Trace amounts of calcium (1.11 wt%) and silicon (0.20 wt%) are discovered, presumably stemming from residual inorganic minerals present in bagasse or injected during activation. The elevated carbon content and oxygen functionality signify effective carbonization while maintaining surface heteroatoms, crucial for adsorption and catalytic performance. The elemental compositions closely correspond with previously documented EDX studies of activated carbons generated from sugarcane, which also exhibit a predominance of C and O, along with trace impurities of Si and Ca [26].

The nitrogen adsorption–desorption isotherm (Figure 5a) displays a type IV pattern with an H3 hysteresis loop, indicative of mesoporous materials [28]. The BJH pore size distribution (Figure 5b) indicates a predominant pore radius of around 2–5 nm, with additional mesopores exceeding 50 nm, so affirming a hierarchical pore structure. The overall pore volume of around 0.14 cm^3 g^{-1} signifies well-developed porosity conducive to adsorption. This porous architecture plays a crucial role in improving Rhodamine B adsorption by increasing the number of accessible sites and facilitating rapid transport of dye molecules into the interior of the adsorbent structure. The BET surface area of 473.766 m^2 g^{-1}, indicating extensive porosity and a high surface area suitable for adsorption applications. These characteristics closely mirror those of previously documented sugarcane-bagasse activated carbons, which also exhibit type IV isotherms and mesoporous distributions conducive to pollutant adsorption.

4.2. RhB adsorption study

The UV-Vis spectra of RhB (Figure 6a) exhibit a gradual decline in the absorption peak at 552 nm as contact time increases, signifying the incremental elimination of dye molecules by the bio-activated carbon sourced from sugarcane bagasse. A substantial decrease in absorbance is noted within the initial 10 minutes, indicating fast adsorption of RhB onto the active sites of the adsorbent. After 20 minutes, only negligible alterations transpire, indicating that equilibrium is almost attained. The associated concentration–time profile (Figure 6b) corroborates this trend, with C_t declining sharply from 10 mg L^{-1} to practically zero, while the removal efficiency (H) swiftly ascends to over 95% within 10 minutes and subsequently stabilizes near 100%. The results underscore the significant affinity and elevated adsorption capacity of bio-activated carbon for RhB, rendering it an exceptionally effective adsorbent for dye-laden wastewater treatment.

Figure 7 illustrates four kinetic models applied to the adsorption of RhB by bio-activated carbon derived from sugarcane bagasse. The pseudo-first-order plot (a) demonstrates a poor fit ($R^2 = 0.703$), suggesting that RhB adsorption does not adhere to a straightforward physisorption-controlled mechanism. Conversely, the pseudo-second-order model (b) demonstrates exceptional linearity ($R^2 = 0.999$), indicating that chemisorption on several active sites is the primary rate-controlling mechanism.

The Elovich figure (c) demonstrates a satisfactory match (R^2 = 0.897), indicating adsorption on a heterogeneous surface characterized by an energetically diverse array of sites. The Bangham analysis (d) produces a slope $\alpha \approx 0.188$ and an intercept $\approx$ -0.247 ($R^2 \approx 0.829$); $\alpha < 1$ indicates that pore (intraparticle) diffusion is a considerable contributor, although it is not the exclusive rate-limiting factor-external film diffusion and surface reaction also exert influence. The adsorption of RhB is optimally characterized by the pseudo-second-order model, incorporating heterogeneous-surface effects and mixed diffusion mechanisms.

Figure 8 depicts the influence of the initial RhB concentration on the removal efficiency (H) of bioactivated carbon obtained from sugarcane bagasse. At low concentrations (5 mg/L), the efficiency is exceptionally high (~98%), indicating a surplus of accessible active sites compared to dye molecules. As the initial concentration escalates from 10 to 25 mg/L, H progressively diminishes to approximately 92%, signifying site saturation and competition among dye molecules for finite adsorption sites. Notwithstanding this reduction, removal efficiency persists over 90%, illustrating the robust adsorption capacity of the bio-activated carbon and its efficacy in effectively removing RhB even at elevated pollutant concentrations.

The adsorption isotherms of RhB on sugarcane-bagasse bio-activated carbon (Figure 9, Table 1) offer significant insights into the adsorption mechanism. The Langmuir model (a) demonstrates a strong match (R^2 = 0.9777) with q_{max} = 30.36 mg g^{-1} and K_L = 1.74 L mg^{-1}, indicating monolayer adsorption on a uniform surface. The Freundlich model (b) exhibits the highest correlation (R^2 = 0.9950), with K_F = 18.02 and n = 1.97 (>1), indicating advantageous multilayer adsorption on heterogeneous sites. The Temkin isotherm (c) (R^2 = 0.9682) signifies a uniform distribution of binding energies and interactions between adsorbate and adsorbent, with K_T = 21.24 and b_T = 6.10 J mol^{-1}. The Elovich model (d) demonstrates a strong match (R^2 = 0.9840), indicating chemisorption on heterogeneous surface sites (α = 78.89 mg g^{-1}, β = 0.0788 g mg^{-1}). The Henry model (e) (R^2 = 0.9396) indicates linear adsorption at low concentrations, whereas the Dubinin–Radushkevich model (f) (R^2 = 0.9306) reveals q_{max} = 20.24 mg g^{-1} and E = 3.63 kJ mol^{-1}, signifying the preponderance of physical adsorption. Adsorption is most accurately characterized by the Freundlich model, which emphasizes heterogeneity and multilayer coverage. The adsorption behavior of Rhodamine B on the prepared activated carbon is governed by a combined physical–surface-controlled mechanism rather than purely chemisorption.

Various agricultural wastes have been investigated as low-cost adsorbents during the previous few decades as shown in Table 2. It can be observed that some materials, such as activated carbon from cotton stalks and palm tree bark, exhibit higher q_{max} values than that obtained in the present study. This variation is mainly attributed to differences in precursor composition, activation method, surface area, and pore structure. Although the maximum adsorption capacity of sugarcane bagasse–derived bio-activated carbon (30.36 mg g^{-1}) is moderate compared with certain reported adsorbents, it demonstrates rapid adsorption kinetics, achieving over

95% dye removal within a short contact time, and maintains high removal efficiency across a wide concentration range. Moreover, the preparation process employs readily available agro-industrial waste and mild activation conditions, contributing to lower production cost and environmental impact. Therefore, rather than outperforming all reported materials in terms of adsorption capacity, sugarcane bagasse-derived bio-activated carbon offers a competitive and sustainable alternative for dye removal, particularly suitable for practical wastewater treatment applications where cost, availability, and treatment efficiency are critical considerations.

5. CONCLUSION

The effective synthesis and application of bio-activated carbon (BAC) derived from sugarcane bagasse for the removal of Rhodamine B (RhB) from aqueous solutions are demonstrated. Comprehensive characterization confirms the formation of a porous carbon structure with abundant surface functional groups and favorable elemental composition, which collectively promote efficient dye adsorption. Batch adsorption experiments indicate rapid uptake, with equilibrium achieved within a short contact time and removal efficiencies exceeding 95% under the investigated conditions. Kinetic analysis shows that the pseudo-second-order model best describes the adsorption process, suggesting surface-controlled adsorption kinetics involving heterogeneous active sites. Isotherm modeling indicates that the Freundlich model provides the best fit, reflecting multilayer adsorption on a heterogeneous surface, while results from other models support the coexistence of physical adsorption mechanisms. Although the adsorption capacity (q_{max} = 30.36 mg g^{-1}) is moderate compared to some reported materials, the use of a sustainable precursor, a simple preparation route, and rapid adsorption behavior highlight the advantages of sugarcane bagasse-derived BAC as a competitive low-cost adsorbent. Further investigation of pH effects and regeneration performance is necessary to fully evaluate its practical applicability in wastewater treatment.

Acknowledgement: *This research was conducted within the framework of the project: "Research on the fabrication of TiO_2/TCPP composite materials based on activated carbon from sugarcane bagasse for application in treating some PFOS/PFOA compounds in aquatic environment" - No. MT.Đ1.15/25. Funding was provided by the Joint Vietnam-Russia Tropical Science and Technology Research Center.*

Statement on the use of Generative AI: *AI tools were used only for language editing and not for generating scientific content. All data, analyses, and interpretations were performed and verified by the authors, who take full responsibility for the manuscript.*

Author contributions: *Nguyen Thi Thu Hang: conceptualization, methodology, investigation, data curation, formal analysis, writing-original draft; Nguyen Kim Thuy: investigation, experimental work, and data collection; Vu Minh Chau: investigation, characterization analysis (SEM, FTIR, XRD); Cao Phuong Anh: data analysis, visualization, and validation; Han Duy Linh: adsorption experiments, kinetic and isotherm modeling; Dang Minh Quang: data interpretation, statistical analysis; Dao Duy Khanh: material characterization support, technical supervision; Duong Tuan Hung: scientific consultation,*

methodology refinement; Nguyen Thi Hoai Phuong: conceptualization, supervision, project administration, funding acquisition, writing review & editing.

Conflict of interest statement: *We have no known competing financial interests or personal relationships that could have influenced the work reported in this paper.*

REFERENCES

1. N. N. Marnani, A. J. C. Shahbazi, *A novel environmental-friendly nanobiocomposite synthesis by EDTA and chitosan functionalized magnetic graphene oxide for high removal of Rhodamine B: Adsorption mechanism and separation property,* Chemosphere, Vol. 218, pp. 715-725, 2019.
2. E. Noman, A. Al-Gheethi, R. M. S. R. Mohamed and B. A. J. T. i. C. C. Talip, *Myco-remediation of xenobiotic organic compounds for a sustainable environment: a critical review,* Topics in Current Chemistry, Vol. 377, No. 3, p. 17, 2019.
3. E. Forgacs, T. Cserháti and G. J. E. i. Oros, *Removal of synthetic dyes from wastewaters: a review,* Environment International, Vol. 30, No. 7, pp. 953-971, 2004.
4. O. J. D. Hamdaoui, *Intensification of the sorption of Rhodamine B from aqueous phase by loquat seeds using ultrasound,* Desalination, Vol. 271, No. 1-3, pp. 279-286, 2011.
5. Q., Lu, W. Gao, J. Du, L. Zhou and Y. Lian, *Discovery of environmental rhodamine B contamination in paprika during the vegetation process,* Journal of agricultural food chemistry, Vol. 60, No. 19, pp. 4773-4778, 2012. DOI: 10.1021/jf300067z
6. S. Jyotshana, S. Shubhangani, B. Upma and S. Vineet, *Toxic effects of Rhodamine B on antioxidant system and photosynthesis of Hydrilla verticillata,* Journal of Hazardous Materials Letters, Vol. 3, No. 100069, 2022. DOI: 10.1016/j.hazl.2022.100069
7. D. Xinxin, G. Leonardo, C. Jean-Philippe, L. Minrui, W. Lijun and W. Yuru, *Hydroxyl and sulfate radical-based oxidation of RhB dye in UV/H2O2 and UV/persulfate systems: Kinetics, mechanisms, and comparison,* Chemosphere, Vol. 253, No. 126655. 2020. DOI: 10.1016/j.chemosphere.2020.126655
8. A.-G. A. Ali, *et al.*, *Sustainable approaches for removing Rhodamine B dye using agricultural waste adsorbents: a review,* Chemosphere, Vol. 287, No. 132080, 2022. DOI: 10.1016/j.chemosphere.2021.132080
9. J. Hu, *et al.*, *Highly-efficient removal of Rhodamine B using a flow-through electrocatalytic filtration system: Characteristics, efficiency and mechanism,* Journal of Electroanalytical Chemistry, Vol. 946, No. 117742, 2023.
10. S. Junaid, S. U. Bin, H. Mouhammad, H. Macke and M. Gordon, *Production and applications of activated carbons as adsorbents from olive stones,* Biomass Conversion Biorefinery, Vol. 9, No. 4, pp. 775-802, 2019. DOI: 10.1007/s13399-019-00473-7
11. L. Di, J. Bao-yu, W. Yun, L. Xia and G. Wen-Yuan, *Effect of activated carbon microstructure and adsorption mechanism on the efficient removal of chlorophyll a and chlorophyll b from Andrographis paniculata extract,* Scientific Reports, Vol. 13, No. 1, p. 21930, 2023. DOI: 10.1038/s41598-023-42011-6
12. P. O. Oladoye, M. Kadhom, I. Khan, K. H. H. Aziz and Y. A. J. G. C. E. Alli, *Advancements in adsorption and photodegradation technologies for Rhodamine B dye wastewater treatment: fundamentals, applications, and future directions,* Green Chemical Engineering, Vol. 5, No. 4, PP. 440-460, 2024.

13. T. Hongyu, *et al.*, *Innovative one-step preparation of activated carbon from low-rank coals activated with oxidized pellets*, Journal of Cleaner Production, Vol. 313, No. 127877, 2021. DOI: 10.1016/j.jclepro.2021.127877
14. V. Strelkov, A. Shirkunov, V. Ryabov and A. Chuchalina, *Granulated activated carbon production based on petroleum coke*. IOP Conference Series: Earth and Environmental Science, IOP Publishing, 2021.
15. F. Mengjiao, *et al., Characteristics of activated carbon from carbonaceous feedstocks of varied origin,* Journal of Environmental Chemical Engineering, Vol. No. 117845, 2025. DOI: 10.1016/j.jece.2025.117845
16. W. A. Khurshid, R. Farida, F. Lilia and S. Cece, *Advances in safe processing of sugarcane and bagasse for the generation of biofuels and bioactive compounds,* Journal of Agriculture Food Research, Vol. 12, No. 100549, 2023. DOI: 10.1016/j.jafr.2023.100549
17. K. Ajay, et al., *Unravelling the potential of sugarcane bagasse: an eco-friendly and inexpensive agro-industrial waste for the production of valuable products using pretreatment processes for sustainable bio-economy,* Journal of Environmental Chemical Engineering, Vol. 12, No. 6, 114461, 2024. DOI: 10.1016/j.jece.2024.114461
18. C. T. Hiranobe, *et al.*, *Sugarcane bagasse: Challenges and opportunities for waste recycling*, Clean technologies, Vol. 6, No. 2, pp. 662-699, 2024. DOI: 10.3390/cleantechnol6020035
19. L.-A. ÁI, *et al.*, *Reutilization of waste biomass from sugarcane bagasse and orange peel to obtain carbon foams: Applications in the metal ions removal,* Science of The Total Environment, Vol. 831, No. 154883, 2022. DOI: 10.1016/j.scitotenv.2022.154883
20. F. Mohamed, *et al.*, *Activated carbon derived from sugarcane and modified with natural zeolite for efficient adsorption of methylene blue dye: experimentally and theoretically approaches,* Scientific Reports, Vol. 12, No. 1, p. 18031, 2022.
21. K. SM, A. NM, I. IM and R. AA, *Activated carbon from sugarcane bagasse pyrolysis for heavy metals adsorption,* Sugar Tech, Vol. 25, No. 3, pp. 619-629, 2023. DOI: 10.1007/s12355-022-01214-3
22. Y. Guo, C. Tan, J. Sun, W. Li, J. Zhang and C. J. C. e. j. Zhao, *Porous activated carbons derived from waste sugarcane bagasse for CO2 adsorption,* Chemical Engineering Journal, Vol. 381, No. 122736, 2020.
23. A. M. Kamal, A. B. Iman and A. S. A. W. Nesrin, *Adsorption of methylene blue onto sugarcane bagasse-based adsorbent materials,* Journal of Physical Organic Chemistry, Vol. 34, No. 7, p. e4193, 2021. DOI: 10.1002/poc.4193
24. R. Vinay, C. M. Singh and P. S. Lal, *Potential of sugarcane bagasse in remediation of heavy metals: A review,* Chemosphere, Vol. 307, No. 135825, 2022. DOI: 10.1016/j.chemosphere.2022.135825
25. P. Lu, Q. Huang, Y. Chi and J. Yan, *Preparation of high catalytic activity biochar from biomass waste for tar conversion,* Journal of Analytical Applied Pyrolysis, Vol. 127, No. 47-56, 2017. DOI: 10.1016/j.jaap.2017.09.003
26. M. Dwiyaniti, L. Krisnawati, A. E. Pramono, A. Subhan, R. Setiabudy and C. Hudaya, *Electrochemical characteristics of sugarcane bagasse-activated carbon as cathode material of lithium-ion capacitors*, Journal of applied research technology, Vol. 21, No. 4, pp. 571-580, 2023. DOI: 10.22201/icat.24486736e.2023.21.4.1976

27. L. Xiao-Yan, *et al.*, *Preparation of a carbon-based solid acid catalyst by sulfonating activated carbon in a chemical reduction process,* Molecules, Vol. 15, No. 10, pp. 7188-7196, 2010. DOI: 10.3390/molecules15107188
28. G. Ze-Long, *et al.*, *The synthesis, characteristics, and application of hierarchical porous materials in carbon dioxide reduction reactions*, Catalysts, Vol. 14, No. 12, p. 936, 2024. DOI: 10.3390/catal14120936
29. Y. Safa, H. N. J. D. Bhatti, *Kinetic and thermodynamic modeling for the removal of Direct Red-31 and Direct Orange-26 dyes from aqueous solutions by rice husk*, Desalination, Vol. 272, No. 1-3, pp. 313-322, 2011.
30. A. Venkatesan, *et al.*, *High adsorption capacities of rhodamine B dye by activated carbon synthesized from cotton stalks agricultural waste by chemical activation,* Ceramics International, Vol. 51, No. 10, pp. 13345-13354, 2025.
31. L. Azeez, et al., *Facile removal of rhodamine B and metronidazole with mesoporous biochar prepared from palm tree biomass: adsorption studies, reusability, and mechanisms*, Water Practice and Technology, Vol. 19, No. 3, pp. 730-744, 2024.
32. Shah, J., M. Rasul Jan, A. Haq and Y. Khan, *Removal of Rhodamine B from aqueous solutions and wastewater by walnut shells: kinetics, equilibrium and thermodynamics studies*, Frontiers of Chemical Science and Engineering, Vol. 7, pp. 428-436, 2013.
33. P. P. Toan, N. T. Thanh and N. T. D. Trang, *Characteristics and adsorption capacity of activated rice husk ash for methyl orange,* Can Tho University Journal of Science, No. 42, pp. 50-57, 2016.

Received: September 10, 2025
Revised: January 12, 2026
Accepted: February 02, 2026